Translational Psychiatry

https://doi.org/10.1038/s41398-026-03821-0

Article in Press

Perinatal hyperandrogenization and immune activation in rodents model subtypes of autism

Received: 17 April 2025

Revised: 12 December 2025

Accepted: 20 January 2026

Cite this article as: Burke, F.F., Randell, A.M., Sparkes, K.M. *et al.* Perinatal hyperandrogenization and immune activation in rodents model subtypes of autism. *Transl Psychiatry* (2026). https://doi.org/10.1038/s41398-026-03821-0

Francine F. Burke, Alison M. Randell, Kerri M. Sparkes, Stephanie Salia, Meagan Hinks, Yellow Martin, Zachary Porter, Claire Hynes, Alexandre S. Maekawa, John Sled, David R. Wilson, Deepak K. Kaushik, Pavan K. Kakumani, Susan G. Walling, Lindsay S. Cahill & Ashlyn Swift-Gallant

Perinatal hyperandrogenization and immune activation in rodents model subtypes of autism

Francine F. Burke[1], Alison M. Randell[1], Kerri M. Sparkes[1], Stephanie Salia[1], Meagan Hinks[1], Yellow Martin[1], Zachary Porter[2], Claire Hynes[3], Alexandre S. Maekawa[2], John Sled[4,5], David R. Wilson[1], Deepak K. Kaushik[2], Pavan K. Kakumani[3], Susan G. Walling[1], Lindsay S. Cahill[6,7], & Ashlyn Swift-Gallant[1*]

1. Department of Psychology, Memorial University of Newfoundland; 232 Elizabeth Ave., St. John's, Newfoundland and Labrador, A1B 3X9, Canada
2. Division of Biomedical Sciences, Faculty of Medicine, Memorial University of Newfoundland; 300 Prince Philip Dr., St. John's, Newfoundland and Labrador, A1B 3V6, Canada
3. Department of Biochemistry, Memorial University of Newfoundland; 45 Arctic Ave., St. John's, Newfoundland and Labrador, A1C 5S7, Canada
4. Mouse Imaging Centre, Hospital for Sick Children; 25 Orde St., Toronto, Ontario, M5T 3H7, Canada
5. Department of Medical Biophysics, University of Toronto; 101 College St., Toronto, Ontario, M5G 1L7, Canada
6. Department of Chemistry, Memorial University of Newfoundland; 45 Arctic Ave., St. John's, Newfoundland and Labrador, A1C 5S7, Canada
7. Discipline of Radiology, Memorial University of Newfoundland; 45 Arctic Ave., St. John's, Newfoundland and Labrador, A1C 5S7, Canada

*Corresponding author: aswiftgallant@mun.ca

Abstract

Although increased maternal androgens, such as those in polycystic ovary syndrome (PCOS), are associated with a higher incidence of autism spectrum disorder (ASD) in offspring, a causal link has yet to be established. We assessed whether perinatal hyperandrogenization in a murine model recapitulates core ASD traits and compared this model to the maternal immune activation (MIA) model of ASD. Both models produced ASD-like phenotypes, yet they exhibited distinct behavioral subtypes and neurodevelopmental trajectories. Hyperandrogenized offspring showed greater reductions in social communication (neonatal USVs, d = 0.633-0.773; juvenile USVs, d = 1.103-1.216; social preference, d = 0.715), whereas only MIA offspring showed increased repetitive behaviors (d = 0.599). *Ex vivo* magnetic resonance imaging revealed volume increases in specific cortical regions in both models, with MIA additionally showing absolute cingulate cortex enlargement, and hyperandrogenized mice displaying focal increases in sexually dimorphic regions, despite a 36% reduction in overall brain volume (FDR 10%). Placentas from both groups showed reduced LIX (CXCL5), but distinct immune shifts also emerged: MIA placentas exhibited elevated IL-4 and IL-1β, whereas hyperandrogenized placentas showed increased TNFα. In neonatal brains, both conditions were associated with reduced IL-2, with MIA additionally decreasing IL-17A and IL-12p70, suggesting suppression of Th1/Th17-type cytokine signaling that normally supports proinflammatory and immune–neural interactions. DRD2 and BDNF protein were upregulated in hyperandrogenized fetal brains but downregulated with MIA. These results suggest that hyperandrogenization and MIA act through distinct mechanisms, producing subtle neurodevelopmental and behavioral differences consistent with human ASD subtypes.

Keywords: Autism Spectrum Disorder; Hyperandrogenization; Maternal Immune Activation; Subgroups; Extreme-Male Brain Theory; Magnetic Resonance Imaging; Neuroinflammation; Pro-inflammatory Cytokines

INTRODUCTION

Neurodevelopmental disorders (NDDs), including autism spectrum disorder (ASD), schizophrenia, and attention-deficit/hyperactivity disorder (ADHD), are characterized by early-onset alterations in cognition, behavior, and brain function. Although these conditions are defined as distinct diagnostic categories, converging evidence from genetics, neuroimaging, and epidemiology indicates substantial overlap in their underlying mechanisms[1–3]. Both genetic and environmental influences shape the likelihood of NDD diagnosis: though heritability is considerable[3–5], factors such as maternal infection, advanced parental age, toxic exposures, autoimmune disease, and pharmaceutical use during pregnancy have also been implicated[6–10]. One of the most consistent factors linked with greater likelihood of diagnosis across NDDs is sex, with males showing higher incidence in several conditions, and most strikingly in ASD, where diagnosis is approximately four times more common in males than females[11].

Several hypotheses have been proposed to explain this sex bias. The *Extreme Male Brain (EMB)* theory describes a male-typical shift in cognition and interests arising from biological, environmental, and/or social factors[12]. By contrast, the *prenatal sex steroid theory* specifically posits that increased prenatal androgen exposure underlies both the male-biased prevalence and associated differences in brain structure, behavior, and, in some studies, morphology[13–15]. Evidence linking higher maternal androgens, such as in polycystic ovary syndrome (PCOS), to greater NDD likelihood supports this view[16–19], although replication across human cohorts has been inconsistent[20,21].

The current study tested whether perinatal hyperandrogenization is sufficient to elicit the core ASD phenotype in male mice by comparing this potential preclinical murine model to the robust maternal immune activation (MIA) model. Featured in more than 930 PubMed indexed

articles (> 630 published over the past five years; *PubMed Search was conducted on July 15, 2024, using the term "maternal immune activation"*), MIA is one of the most studied environmentally-induced preclinical rodent models of NDD[22], likely due to its high construct, predictive, and face validity[23,24], specifically: 1) Maternal infection or heightened immune reactivity, such as in autoimmune conditions, increases the risk of ASD in humans, with an estimated 12% higher probability[6,9,25,26] (but see [27] for alternative interpretation). 2) An ASD-like phenotype is apparent in rodent MIA offspring through an array of behavioral tests for social communication (SC; e.g., reduced ultrasonic vocalizations in response to maternal separation; decreased preference for sociability and social novelty preference in a three chambered test), and restricted and / or repetitive behaviors (RRB; e.g., increased marble burying and/or repetitive grooming)[24,28–30]. 3) Rodent MIA offspring experience changes in proinflammatory cytokine activity and neuroimmune activation (e.g., microglia) that parallel those observed in the human condition[31,32]. Finally, 4) rodent models of MIA demonstrate a sex bias like in the human condition, where compared to females, male offspring are more likely to show ASD-like symptomology (e.g., [29,33]).

By directly comparing perinatal hyperandrogenization to the MIA model, and their combination, we also assessed whether these mechanisms (hyperandrogenization and/or MIA) lead to particular phenotypic presentations, linking mechanisms to heterogeneity in phenotype. Investigation into potential subgroups of the human condition has either supported 1) a continuous spectrum where individuals differ only in severity of symptoms, or 2) three subgroups, based on the two primary diagnostic criteria, SC and RRB; one subtype is highly affected across both domains (SC = RRB), and two less severe groups, each distinguished by one domain being more pronounced than the other (SC > RRB, SC < RRB[34,35]). We evaluated

whether MIA and hyperandrogenization support a continuous spectrum of symptoms (e.g., MIA > hyperandrogenization > MIA + hyperandrogenization), distinct subgroups (e.g., MIA = SC < RRB, hyperandrogenization = SC > RRB, and MIA + hyperandrogenization SC = RRB), or equifinality (i.e., different causal mechanisms leading to similar endpoints)[2,36]. Maternal, placental, and brain analyses across fetal, neonatal, and juvenile development were also conducted to assess whether inflammation, gene expression and neuroanatomical changes are unique to each model (Fig. 1). These measures were performed to determine if the developmental trajectory and mechanisms differed for each exposure.

MATERIALS AND METHODS

Animals

Wildtype C57BL/6-N mice were obtained for breeding (see EM for details) from Charles River Laboratories (St. Constant, QC, Canada). Ethical approval was obtained from the Institutional Animal Care Committee at Memorial University of Newfoundland and Labrador, and animal use was conducted following the Canadian Council on Animal Care (CCAC) guidelines.

MIA and androgen treatment

MIA was induced in pregnant dams through intraperitoneal (IP) administration of polyinosinic:polycytidylic acid (poly I:C; Sigma-Aldrich; 1.25 mg / mL of 0.9% NaCl) at a dose of 5 mg/kg on embryonic day (E) 17.5. Testosterone propionate (TP; Steraloids Cat# A7000-000; 1 mg/mL of corn oil) was administered subcutaneously to pregnant dams on E16, 18, and 20, and to pups on the first day of birth [postnatal day (PND) 1] at a volume of 0.1 mL. Controls received vehicle injections of the same volumes.

Behavior

Neonatal isolation USVs were assessed at PND 4, 6, and 8, and a behavioral battery assessing communication, social, and repetitive behavior was performed at the juvenile stage (i.e., PND 35–45). See extended methods (EM) for details. We selected the juvenile stage because most MIA research evaluates behavior during this period, where alterations are well-documented.[24, 28-30] Evidence also suggests that MIA-induced social abnormalities are particularly robust in juveniles and adolescents, but tend to be subtler in adulthood[37].

Tissue collection

On the day following the last behavioral test (PND 43-45), mice were weighed, overdosed with Avertin (40 mg / kg) via IP injection, and decapitated. Trunk blood was collected and centrifuged at 2000 rpm at 4°C for 20 minutes. Serum was collected from the supernatant and stored at -20°C. Brain tissue was post-fixed in 4% paraformaldehyde for 4 hours, transferred to 20% sucrose, and refrigerated until sectioning. Brains were sectioned on a sliding freezing microtome at 30 μm and stored in cryoprotectant at -20°C.

Immunohistochemistry and stereology

To characterize microglia in the hippocampal dentate gyrus (DG) of juvenile offspring, immunohistochemistry for Iba-1 (1:10,000 Iba-1 anti-rabbit, Wako Chemicals, Cat# 019-19741), was conducted as detailed in EM. Stereology was performed by a blinded investigator using a Leica DM6 microscope and Stereologer® Software (SRC Biosciences, Tampa, FL) to measure microglial cell size, cell count, process length, and DG volume.

***Ex vivo* magnetic resonance imaging (MRI)**

On PND 45, juvenile males were transcardially perfused, and tissue was prepared as previously described[38]. Images were acquired on a 7 Tesla, 306 mm horizontal bore magnet (BioSpec 70/30 USR, Bruker, Ettlingen, Germany)[39,40], detailed in EM. Multiple comparisons

were controlled for using the false discovery rate (FDR) and statistical significance was defined as an FDR threshold of 15%, however, 5% and 10% FDR are also reported in Table 1.

Quantification of maternal and offspring cytokines & gene expression

On E18.5, dams were overdosed with Avetin (40 mg / kg) via IP injection and decapitated. Trunk blood of dams was collected and centrifuged at 2000 rpm for 20 minutes at 4°C. Serum was collected and stored at -20°C. Presumed male fetuses and placentas were removed from the uterine horn and their brains were extracted and flash-frozen using 2-methylbutane on dry ice and stored at -80°C until use; sex was later confirmed via genotyping for the sex-determining region of the Y-chromosome (*Sry*, primers reported in EM Table 1).

Male pups were euthanized on PND 1 via rapid decapitation. Brains were extracted, flash-frozen, and stored at -80°C. To homogenize tissue, digestion buffer was prepared using Pierce RIPA Buffer (Cat. 89900) and Halt Protease and Phosphatase inhibitor (Cat. 1861281 100X) at a final concentration of 1x. An 18-plex assay (MDHSTC18) was conducted by Eve Technologies (Calgary, Alberta, Canada). Samples were tested in duplicate, and the observed concentrations (pg / mL) were averaged. See EM for RT-qPCR details and ED Table 2 for primers. The genes selected for RT-qPCR analysis were chosen based on their established relevance to NDDs. IL-1β, IL6, and TNFα are key proinflammatory cytokines frequently elevated in MIA models and in individuals with ASD, reflecting neuroimmune dysregulation[41]. Iba-1 serves as a marker of microglia, which are neural immune cells, implicated in both prenatal inflammation and altered synaptic pruning in ASD[42–44]. Gad1 encodes glutamate decarboxylase, a critical enzyme in GABA synthesis, and has been linked to excitation-inhibition imbalance in ASD[45]. DRD2 and Grin2a, representing dopaminergic and glutamatergic signaling respectively, are involved in reward processing and synaptic plasticity, both of which are altered in ASD[46,47].

BDNF is a neurotrophic factor essential for neuronal growth and synaptic development, and its dysregulation has been observed in ASD and MIA contexts[48–50]. Akt1 is a key signaling molecule downstream of BDNF and other growth factors and has been implicated in neurodevelopmental trajectories[51]. β-actin was used as a housekeeping gene for normalization.

For western blots (WB), polyclonal antibodies for Gad1 (cat# 10408-1-AP), BDNF (cat# 28205-1-AP), and DRD2 (cat# 55084-1-AP) were acquired from Proteintech Group, Inc. β-actin was used as a loading control, by placing sections of the nitrocellulose membrane in a 1:25000 antibody solution (HRP-conjugated β-actin monoclonal antibody (Proteintech Group, Inc., cat# HRP-66009) in 1% BSA in 1X PBS-T. For further details on WB, see EM.

Steroid hormones

Trunk blood was collected from neonatal males at time of euthanasia (PND 1) and centrifuged at 2000 rpm at 4°C for 20 minutes. Serum was collected from the supernatant and stored at -20°C and processed on the hormone array (STTHD-Serum-Plasma Array) by Eve Technologies (Calgary, Alberta, Canada). Samples were tested in duplicate, and the observed concentrations (ng / mL) were averaged.

Statistical analysis

Between-subjects Analysis of Variance (ANOVA) was used to compare groups on somatic measures, social behavior, and microglia data. Marble burying was analysed with a repeated-measures ANOVA. Neonatal and juvenile USVs were analysed using multivariate ANOVA (Pillai's Trace). When the multivariate test was significant, follow-up univariate ANOVAs were conducted. Principal components analysis (PCA) was used to analyze cytokine profiles, with oblimin rotation and an eigenvalue cutoff of 1. Groups were compared on component scores with ANOVA; when significant, individual cytokines of such components with

loadings greater than 0.4[52,53] were followed up with individual cytokine analysis using ANOVA. For MRI results, multiple comparisons were controlled for using false discovery rate (FDR) and statistical significance was defined as an FDR threshold of 15%, however more stringent FDR's of 5% and 10% are also reported (see Table 1). Across all analyses, significance was set at $\alpha = .05$. For significant ANOVAs, post-hoc comparisons using Fisher's LSD were conducted. Intraclass correlation coefficients (ICC) were calculated for behavioral measures with two or more raters (See EM). All statistical analyses were performed using Jamovi software (Version 2.3.18; retrieved from https://www.jamovi.org), unless otherwise noted.

RESULTS

MIA and perinatal hyperandrogenization altered communication across development

Neonates

Mouse pups produce ultrasonic vocalizations (USVs) to elicit a retrieval response from dams and / or to encourage feeding and grooming[54]. We recorded USVs at PND 4, 6, and 8 (N = 45-51, n = 9-13 / group) in response to a three-minute separation from the nest[55]. At PND 4, no significant effects were detected. At PND 6, hormone treatment affected USVs, with hyperandrogenized pups exhibiting higher average call frequencies than controls ($d = 0.633$; Fig. 2c). At PND 8, hyperandrogenized pups had higher average call frequency ($d = 0.773$; Fig. 2c), reduced call number ($d = 0.741$; Fig. 2a), and shorter total call duration ($d = 0.733$; Fig. 2b) relative to controls.

Juveniles

As juveniles (N = 41, n = 9-12 / group), MIA and hyperandrogenization independently decreased total calls (same-sex: $d = 1.226, 1.216$; opposite-sex: $d = 0.950, 1.207$; Fig. 2d) and time spent calling (same-sex: $d = 1.178, 1.139$; opposite-sex: $d = 0.892, 1.103$; Fig. 2e) while

encountering a stimulus of either sex. Call frequency (Fig. 2f) and call types (ED Fig. 1b) were not affected by MIA or hyperandrogenization. Hyperandrogenization in combination with MIA did not differ from MIA or hyperandrogenization alone in juvenile communication measures.

Perinatal hyperandrogenization produced greater atypical social behavior than MIA

Atypical patterns of social behaviour in rodent models of ASD are characterized by a decrease in sociability (i.e., the tendency to spend time with a conspecific as opposed to spending time alone) and social novelty preference (i.e., the tendency to investigate an unfamiliar rather than a familiar conspecific), using a three-chamber social paradigm (Fig. 2g; N = 49, n = 12-13 / group)[28,29].

Hyperandrogenization alone led to decreases in the sociability index (d = 0.715; Fig. 2h), reflective of less time spent in the social chamber and increased time in the non-social chamber compared to controls (d = 0.665; Fig. 2i). MIA offspring did not differ in duration of time with the social stimulus or in the sociability index compared to controls. In the social novelty phase, MIA offspring had a reduced social novelty score (d = 0.781; Fig. 2h), as they spent less time in the novel stimulus chamber (d = 0.761) and more time in the familiar stimulus chamber than controls (d = 0.727; Fig. 2j). Conversely, hyperandrogenized animals spent more time in the novel stimulus chamber (d = 0.714) and less time in the familiar stimulus chamber (d = 1.135) than controls. See ED Fig. 2 for time and entries in interaction zones.

MIA, but not hyperandrogenization, increased repetitive marble burying

To assess repetitive behavior (N = 49, n = 12-13 / group), we implemented a 30-minute marble-burying task[28]. MIA offspring buried more marbles than controls at the 10-minute timepoint (d = 0.599), while hyperandrogenization did not differ from controls on any measure (Fig. 2k).

Reduced total brain volume with relative increases in cortices in hyperandrogenized male mice

MRI analyses (N = 24, n = 8 / group) revealed that whole brain volume was 3.9% smaller in hyperandrogenized than control mice ($p = 0.008$). Indeed, 2% (4/182), 18% (32/182) and 40% (72/182) of segmented brain structures were significantly smaller in the hyperandrogenized than control male brains at 5%, 10% and 15% FDR (see Table 1). However, when controlling for brain volume, several focal increases were found in the hyperandrogenized mice than controls, including in the nucleus accumbens (NA), bed nucleus of the stria terminalis (BNST), and motor cortices (Fig. 3). In contrast, MIA mice differed from controls with regional increases in the relative volume of the cingulate cortex and motor cortices.

Immunology and endocrinology profiles

MIA and hyperandrogenization uniquely influenced maternal and offspring cytokines

An 18-plex high-sensitivity proinflammatory panel was used to evaluate immune activity in dam serum (N = 13, n = 3-6 / group), placenta (N = 20, n = 6-7 / group), and fetal brains (N = 21, n = 7 / group) at E18.5, and neonatal brains (N = 15, n = 5 / group) on the day of birth (Fig. 4a). PCA of dam serum and fetal brains did not reveal significant group differences in component scores. In placentas (Fig. 4b), Component 2 scores were reduced in both hyperandrogenized ($d = 1.294$) and MIA ($d = 2.337$) placentas compared to controls, driven primarily by LIX, KC, IL-4, and IL-1β. Follow-up analyses showed reduced LIX in both hyperandrogenized ($d = 1.511$) and MIA ($d = 1.383$) placentas, and elevated IL-4 in MIA placentas ($d = 1.515$), relative to controls. IL-1β was increased in MIA placentas relative to hyperandrogenized ($d = 1.417$) and control ($d = 1.517$) placentas. Component 3 scores were higher in MIA placentas compared to hyperandrogenized placentas ($d = 1.493$), with

contributions from TNFα, MIP-2, IL-10, IL-5, IL-4, and IFNγ. Follow-up analyses showed elevated TNFα in hyperandrogenized placentas relative to MIA placentas (d = 1.606). Component 4 scores were higher in hyperandrogenized placentas (d = 1.540). TNFα, IL-10, IL-6, and IL-2 contributed to this component, primarily reflecting increased TNFα relative to MIA placentas (d = 1.606). In neonatal brains (Fig. 4c), Component 1 scores were elevated in both hyperandrogenized (d = 1.958) and MIA (d = 2.204) neonates relative to controls, with contributions from TNFα, MIP-2, IL-2, IL-4, IL-17A, and IL-12p70. Follow-up analyses found reduced IL-2 in both hyperandrogenized (d = 2.089) and MIA pups (d = 2.205) and reduced IL-17A and IL-12p70 in MIA pups (d = 1.770, 1.696) relative to controls.

Increased microglial activation in DG with hyperandrogenization but not MIA

Microglia via Iba-1 immunohistochemistry (N = 15, n = 4-6/group) were assessed in the hippocampal dentate gyrus (DG), a region implicated in ASD rodent models and the human condition (e.g., [56–58]). Using stereology, Iba-1 positive cells were assessed for number, nucleus size, and process length (Fig. 4d). Microglia in the DG of hyperandrogenized males were found to have shorter processes than those of MIA (d = 2.126) and controls (d = 1.643). The density of microglia in DG was reduced in hyperandrogenized animals compared to MIA (d = 1.924), while both groups were comparable in DG volume.

BDNF and DRD2 are upregulated with hyperandrogenization, but downregulated with MIA

RT-qPCR was performed to assess mRNA expression of the following genes in fetal (N = 21, n = 7 / group) and neonatal (N = 15, n = 5 / group) male brains: IL-1β, IL-6, TNF-α, Gad1, DRD2, BDNF, GRIN2A, Akt1, and Iba-1; while no significant differences were found between groups at either the fetal or neonatal stage (ED Table 1; ED Fig. 3), it was noted that the variability was quite high in treatment groups for Gad1, BDNF, and DRD2. Western blots were

conducted on fetal and neonate brains for these three proteins of genes that had the highest variation. Hyperandrogenized fetal & neonate brains exhibited greater BDNF and DRD2 protein than MIA and controls, while MIA fetal & neonate brains showed a reduction in both BDNF and DRD2 than controls (Fig. 4e). Groups did not differ for Gad1.

Prenatal hyperandrogenization, but not MIA, raised serum cortisol in neonates

A steroid hormone panel including testosterone (T), progesterone (P4), estradiol (E2), cortisol, triiodothyronine (T3), and thyroxine (T4) was conducted on neonatal serum (PND 1; N = 12, n = 3 samples / group – each sample included serum from 2-4 pups), as increased fetal androgenic activity[59] and serum cortisol[60] have been found to be elevated in ASD children. Prenatal androgen treatment did not alter serum T on PND 1; however, altered T was not necessarily predicted, as mice euthanized on PND 1 were last administered T on E18. Serum cortisol was elevated in hyperandrogenized, but not MIA, offspring compared to controls (d = 4.786; Fig. 4f). Although P4 did not differ in group comparisons, a positive correlation was found between P4 and cortisol (r = 0.683, p = .042).

DISCUSSION

We investigated perinatal hyperandrogenization as a preclinical mouse model of ASD and compared this to the well-established MIA model. Hyperandrogenization produced greater alterations in social communication than MIA, whereas MIA, but not hyperandrogenization, increased RRB. Unexpectedly, hyperandrogenization in combination with MIA did not exacerbate ASD-like behaviors. Although both models display ASD-like phenotypes, they present with distinct behavioral, immunological, endocrinological, and neuroanatomical profiles, suggesting that MIA and hyperandrogenization act via distinct neurodevelopmental pathways to produce ASD subtypes. The distinction in SC and RRB phenotypes map onto the replicable subgroupings in the human population, with hyperandrogenization resembling the SC > RRB subgroup, and MIA the SC < RRB subgroup[34]. Given the heterogeneity of ASD in both symptom presentation and etiological factors, this work highlights how preclinical rodent models can provide insights into mechanisms driving distinct subtypes and help identify biomarkers for subtype delineation in humans. These findings underscore a potential mechanism contributing to the sex bias in ASD: because males are naturally exposed to higher androgen concentrations than females, even subtle variations – such as increased endogenous production, reduced sex hormone-binding globulin, heightened receptor sensitivity, or elevated maternal sources, may be sufficient to promote ASD development in males.

As one of the earliest measures of communicative behavior in mice, neonatal USVs are an essential means of assessing an ASD-like phenotype[61,62]. Further, USVs in juveniles serve as a critical means of conveying socially relevant information to conspecifics and are correlated with bonding and motivation[63,64]. Here, we find that perinatal hyperandrogenization produced more widespread alterations in the neonatal period than MIA, with similar alterations in USV

production to MIA in juvenile measures. Ultrasonic communication after perinatal hyperandrogenization has not previously been assessed in mice to our knowledge, however, these findings are consistent with rats exposed to a hyperandrogenic intrauterine environment due to dam letrozole treatment[65] and a rat model of PCOS[66].

Social behaviors further highlight subtype-specific effects. We replicated the finding that MIA offspring exhibit decreased social novelty preference compared to controls[28,29]; however, more pronounced social alterations were observed in the perinatal hyperandrogenization model. Hyperandrogenized offspring showed reduced sociability, while social novelty preference was increased relative to controls. In the three-chamber test, the sociability phase primarily reflects general social approach, whereas the social novelty phase engages social memory and recognition[67]. These results suggest that MIA primarily affects social recognition, whereas hyperandrogenization leads to broader alterations in social behavior, with social memory appearing relatively preserved or enhanced.

We replicated the finding of increased repetitive behavior in MIA offspring using the marble burying test[28,29]. In contrast, perinatal hyperandrogenization did not increase RRB. These results support the use of perinatal hyperandrogenization as a model for the SC > RRB subtype of ASD, whereas MIA more closely resembles the SC < RRB profile. Notably, we classify MIA as SC < RRB rather than SC = RRB because the latter in humans typically refers to individuals with atypical patterns in both domains[35], whereas MIA offspring in this study show relatively mild impairments in social communication.

We also find evidence of increased neuroinflammation in the hyperandrogenization, but not the MIA, model. Neuroinflammation, including activated microglia, has been reported in ASD individuals (reviewed in [44,68]). Findings on microglial alterations in MIA are mixed (e.g.,

[42,69–71]), which may reflect differences in the timing of immune activation: For example, Ozaki et al. (2020)[42] found that MIA induced in early gestation (E12) produced long-lasting changes in microglial processes in the somatosensory cortex, whereas mid-gestation induction (E15) did not alter microglial activation. Because MIA in our study was induced in late gestation, this may partly explain the absence of microglial differences. In contrast, hyperandrogenized mice showed reduced microglial dendritic extent and density in the hippocampal DG relative to controls. The shorter process length suggests an activated / amoeboid phenotype, which, when chronic, can lead to neuronal cell death (reviewed in [72,73]). Microglia were assessed in the juvenile period, more than six weeks after treatment, suggesting that the activated state is persistent. Our MRI results, discussed further below, indicate overall reductions in brain volume, which may partly reflect overactive microglia causing increased apoptosis, phagocytosis of neurons, and production of neurotoxic factors (reviewed in [74]). Interestingly, increased activated / amoeboid microglia has been reported among adult offspring in rodent models of PCOS[75], supporting the idea that elevated prenatal androgen exposure can have long-lasting effects on the neuroinflammatory state of offspring.

Both BDNF and DRD2 have been implicated in ASD development[47,49,76], and here we find that both are upregulated in the hyperandrogenization model but downregulated in MIA (note: consistent with previous reports of MIA and BDNF: [50,77], and MIA and DRD2: [78,79]). Altered BDNF, a critical neurotrophic factor supporting neuronal survival, growth, differentiation, plasticity, and cognitive function, is frequently reported in individuals with ASD, but findings are mixed, with studies showing elevated, reduced, or unchanged blood levels compared to controls[76,80,81]. Our results suggest that these conflicting reports may reflect differences between SC > RRB (hyperandrogenization) and SC < RRB (MIA) subtypes. This

result is further supported by the role of androgens in regulating BDNF: ER and AR signaling can increase neural and peripheral BDNF expression[82–84]. Similarly, dopamine transmission is androgen-sensitive[85], and mutations in dopamine receptor genes are associated with ASD in humans[47,86,87] and ASD-like phenotypes in rodent models[88–90]. Further, there are indications that mutations in DRD2 may increase the likelihood of ASD in families with only male members affected[87]. While our RT-qPCR targets were selected based on known associations with ASD and MIA-related pathways, we acknowledge that this hypothesis-driven approach limits broader transcriptomic discovery, and future studies using RNA-sequencing could provide a more comprehensive view of gene expression changes. Nevertheless, our findings suggest heterogeneity in BDNF and DRD2 expression in ASD may reflect opposing patterns across subtypes, with upregulation in SC > RRB and downregulation in SC < RRB.

Despite heterogeneity in ASD neuroanatomy, enlarged cortical regions are a consistent feature in many populations (e.g., [91,92]). In our MRI analysis, both MIA and hyperandrogenized offspring showed relative enlargement of primary and secondary cortices, with MIA brains also exhibiting an enlarged cingulate cortex. Hyperandrogenization, however, produced an overall 3.9% reduction in brain volume across 40% of regions, alongside focal increases in the NA and anterior BNST. Enlarged cortices align with human ASD findings[92–94], and cingulate involvement has been linked to repetitive behaviors[95,96] consistent with the greater RRB phenotype in the MIA model. The NA and BNST increases in hyperandrogenized mice are notable given their roles in social communication[97–105] and sexual dimorphism[106,107], supporting a contribution of prenatal androgens to their differentiation. These structural patterns may underlie the relatively greater social-communication atypicalities in the hyperandrogenization model and the stronger RRB phenotype in the MIA model. While males typically have larger

brains than females, the overall brain volume reduction with hyperandrogenization is consistent with prior evidence of a U-shaped relationship between androgen signaling and male-typical phenotypes[108]. These findings may also align with recent reports of smaller brain volume at birth in children later exhibiting high autistic traits, suggesting that cortical overgrowth in ASD may occur postnatally[109].

During MIA, maternal cytokines can affect the fetus via amniotic fluid, plasma, and placenta, potentially exerting lasting effects on the CNS[29,110]. Both MIA and hyperandrogenization produced overlapping and model-specific inflammatory changes in placenta and neonatal brain (Fig. 5). In both models, reduced placental LIX (CXCL5) may impair immune cell recruitment, affecting trophoblast invasion, nutrient transfer, and local cytokine gradients critical for brain development[111,112]. MIA uniquely elevated IL-1β and IL-4, suggesting proinflammatory signaling that could alter placental vascularization, barrier function, or prime fetal microglia[113,114], whereas hyperandrogenization increased TNFα, potentially activating stress or apoptotic pathways and indirectly influencing neurogenesis and synaptogenesis[115]. Neonatal brains reflected these placental shifts: both models showed increased TNFα, MIP-2, and IL-4, alongside reduced IL-2, with additional IL-17A and IL-12p70 decreases in MIA. These patterns indicate suppression of Th1/Th17 signaling, which normally drives cellular immunity and pathogen clearance, among MIA offspring, possibly reducing immune activation but also compromising neuroprotective mechanisms[116]. IL-2, a pleiotropic cytokine with anti- and pro-inflammatory roles and neuroprotective effects[117,118], was reduced in both models, suggesting loss of protective signaling. Such shifts may represent compensatory attempts to limit inflammation but could leave developing circuits vulnerable to stress and excitatory–inhibitory imbalance.

Lastly, we examined effects of MIA and androgenization in females (see EM). Offspring from androgenized dams are referred to as "androgenized" rather than "hyperandrogenized," as the dose partially masculinizes females but remains below male-typical levels (e.g., they are clearly distinguishable from males in anogenital distance and phenotype). MIA effects in females largely mirrored those in males but were less pronounced. Androgenization did not increase ASD-like behaviors. Neither MIA nor androgenization altered the number or duration of calls in neonatal females or in juveniles interacting with male or female conspecifics, suggesting female social communication may be relatively resilient to prenatal androgen or immune challenges. MIA females showed greater RRB on marble burying, whereas androgenized MIA females buried fewer marbles, indicating androgens attenuated MIA effects on RRB. No clear effects were observed on sociability or social novelty. Overall, MIA females exhibited modest changes in social communication and RRB, while androgenization altered USV call frequency but did not increase ASD-like behaviors. Unexpectedly, androgenization appeared protective against some MIA effects, particularly RRB.

In humans, excess androgen exposure during gestation has been linked to elevated cytokine levels implicated in ASD pathophysiology[119]. Individuals with PCOS, who often experience hyperandrogenism and chronic low-grade inflammation during pregnancy, are up to 60% more likely to have a child with ASD than those without PCOS[120–124]. Similarly, preeclampsia—a hypertensive disorder associated with increased testosterone—is also associated with increased odds of having a child with ASD[125,126]. These converging lines of evidence suggest that elevated maternal androgens can increase inflammation and ASD risk in humans, and here, we present a murine model of hyperandrogenization in which maternal androgen levels were experimentally increased, producing ASD-like phenotypes in offspring. However, it is

important to note the differences between species in terms of both pregnancy and sexual differentiation. For instance, although both humans and rodents have hemochorial placentas, there are notable differences in placental architecture, hormone production, and immune signaling; for example, the rodent placenta has a distinct labyrinth zone and relies more on trophoblast invasion for nutrient exchange, whereas the human placenta features a more complex villous structure and prolonged gestational endocrine regulation[127,128]. Sex differentiation mechanisms also differ; though both species rely on SRY to initiate testis development and mid-late gestation androgen secretion, the timing, hormonal environment, and downstream gene regulation vary, potentially altering the developmental impact of prenatal exposures[129].

Limitations and Future Directions

While the current work has been interpreted within the context of available research, several methodological and biological considerations are important for guiding future studies. For instance, interpretation of USV data should consider the possible influence of non-central nervous system factors, such as body size, physiology, and the development of vocal musculature. Attributes such as lung capacity and laryngeal maturation can affect USV frequency, amplitude, and duration independently of central nervous system control[130]. Future work could use techniques like micro-CT to assess these contributions.

Serum testosterone was not elevated at PND1 in offspring exposed to T on ED18, consistent with human studies showing no significant steroid increases in the cord blood of autistic individuals[131,132]. This may reflect rapid placental aromatization of testosterone to estradiol, a key mechanism regulating fetal hormone exposure[59]. Future studies should assess placental aromatase activity to determine how this conversion influences the developmental effects of prenatal androgen exposure. Moreover, the pronounced pro-inflammatory response at

the placenta suggests that this site could serve as a promising target for future intervention or rescue experiments.

Perinatal hyperandrogenization and MIA also reduced testis, seminal vesicle, and body weights, indicating potential disruptions to hypothalamic-pituitary-gonadal (HPG) axis function. Such alterations could lead to changes in circulating hormone levels during juvenile development, which may influence behavioral outcomes. Consequently, the behavioral phenotypes observed might reflect a combination of direct neurodevelopmental effects from MIA and indirect effects mediated by altered hormone signaling via HPG axis disruptions. Future studies should disentangle hormonal versus neural contributions to these behaviors.

Finally, the hormone assay panel used in this study measured cortisol rather than corticosterone. Because corticosterone is the primary glucocorticoid in mice, measuring it would provide a more accurate assessment of HPA axis function.

Translational Considerations

Consideration of translational relevance is essential when interpreting the findings presented here. Murine hyperandrogenization and maternal immune activation models capture specific neurodevelopmental and behavioral features relevant to ASD, but they do not reflect the full clinical heterogeneity of the condition. ASD varies widely in symptom presentation and underlying etiology, limiting the generalizability of results from animal models to the broader population. In addition, experimental manipulations of maternal androgens or immune activation in rodents involve highly controlled interventions that cannot fully replicate the complex genetic, environmental, and developmental interactions contributing to ASD risk in humans. Although the present findings provide insight into model-specific neuroimmune and behavioral alterations, caution is warranted when extrapolating to human clinical contexts. These data should be

interpreted as preclinical evidence that informs understanding of neurodevelopmental mechanisms and underscores the need for further translational and clinical validation.

Conclusion

The current studies comprehensively characterized a perinatal hyperandrogenization model for ASD, and by directly comparing this model to the well-established MIA preclinical ASD model, we: 1) demonstrated that exposure to excess androgens during perinatal development is sufficient to induce ASD-like symptomology in offspring, 2) identified distinct differences in biological markers indicative of ASD-like development following perinatal hyperandrogenization, and 3) discerned that MIA and perinatal hyperandrogenization have differential etiologies and correspond to different ASD SC vs RRB subtypes. Our findings underscore the importance of using multiple rodent models to study ASD subgroups and causal mechanisms to phenotype connections, and we recommend the perinatal hyperandrogenization model as an addition to the repertoire of preclinical mouse models for studying ASD.

Acknowledgements

We thank Animal Care Services at Memorial University of Newfoundland for their assistance with animal husbandry; Eve Technologies for their assistance in cytokine and hormone assays; Mouse Imaging Centre at the Hospital for Sick Children in Toronto, Ontario for performing juvenile brain MRIs.

Funding

Canadian Institutes of Health Research (CIHR) project grant 495842 (ASG).

Natural Sciences and Engineering Research Council of Canada (NSERC) Discovery Grant RGPIN-2019-04999 (ASG).

Author contributions

Conceptualization: FFB, ASG

Behavior: FFB, KMS, AMR, YM, SS, MH

Ultrasonic vocalization analyses: FFB, DRW, SS, AMR

Immunohistochemistry: FFB, AMR, SGW, ASG

Microscopy: FFB, AMR

Western blotting & qPCR: CH, PKK

Cytokine analyses: FFB, AMR, ZP, DKK, ASM

Genotyping: ASM

MRI: AMR, JS, LSC

Data analysis: FFB, LSC, AMR, ASM, CH, DW, PKK, SGW, ASG

Writing – original draft: FFB, ASG

Writing – review & editing: All authors

Competing interests

The authors declare no competing interests.

Data availability

All data associated with this study are present in the main text or the supplementary materials.

References

1 American Psychiatric Association, American Psychiatric Association DSM-5 Task Force. *Diagnostic and statistical manual of mental disorders: DSM-5.* Fifth edition. American Psychiatric Association: Arlington, VA;, 2013.

2 Bertelsen N, Landi I, Bethlehem RAI, Seidlitz J, Busuoli EM, Mandelli V *et al.* Imbalanced social-communicative and restricted repetitive behavior subtypes of autism spectrum disorder exhibit different neural circuitry. *Commun Biol* 2021; **4**: 574.

3 Havdahl A, Niarchou M, Starnawska A, Uddin M, Merwe C van der, Warrier V. Genetic contributions to autism spectrum disorder. *Psychol Med* 2021; **51**: 2260–2273.

4 Rylaarsdam L, Guemez-Gamboa A. Genetic Causes and Modifiers of Autism Spectrum Disorder. *Front Cell Neurosci* 2019; **13**: 385.

5 Hallmayer J, Cleveland S, Torres A, Phillips J, Cohen B, Torigoe T *et al.* Genetic Heritability and Shared Environmental Factors Among Twin Pairs With Autism. *Arch Gen Psychiatry* 2011; **68**: 1095–1102.

6 Jiang H, Xu L, Shao L, Xia R, Yu Z, Ling Z *et al.* Maternal infection during pregnancy and risk of autism spectrum disorders: A systematic review and meta-analysis. *Brain Behav Immun* 2016; **58**: 165–172.

7 Wu S, Wu F, Ding Y, Hou J, Bi J, Zhang Z. Advanced parental age and autism risk in children: a systematic review and meta-analysis. *Acta Psychiatr Scand* 2017; **135**: 29–41.

8 Dutheil F, Comptour A, Morlon R, Mermillod M, Pereira B, Baker JS *et al.* Autism spectrum disorder and air pollution: A systematic review and meta-analysis. *Environ Pollut* 2021; **278**: 116856.

9 Chen S, Zhong X, Jiang L, Zheng X, Xiong Y, Ma S *et al.* Maternal autoimmune diseases and the risk of autism spectrum disorders in offspring: A systematic review and meta-analysis. *Behav Brain Res* 2016; **296**: 61–69.

10 Bölte S, Girdler S, Marschik PB. The contribution of environmental exposure to the etiology of autism spectrum disorder. *Cell Mol Life Sci CMLS* 2018; **76**: 1275–1297.

11 Loomes R, Hull L, Mandy WPL. What Is the Male-to-Female Ratio in Autism Spectrum Disorder? A Systematic Review and Meta-Analysis. *J Am Acad Child Adolesc Psychiatry* 2017; **56**: 466–474.

12 Baron-Cohen S. The extreme male brain theory of autism. *Trends Cogn Sci* 2002; **6**: 248–254.

13 Bakker J, Mees CD, Douhard Q, Balthazart J, Gabant P, Szpirer J *et al.* Alpha-fetoprotein protects the developing female mouse brain from masculinization and defeminization by estrogens. *Nat Neurosci* 2006; **9**: 220–227.

14 Phoenix CH. Organizing action of prenatally administered testosterone propionate on the Tissues mediating mating behavior in the female guinea pig. *Horm Behav* 2009; **55**: 566–566.

15 Zuloaga DG, Puts DA, Jordan CL, Breedlove SM. The role of androgen receptors in the masculinization of brain and behavior: What we've learned from the testicular feminization mutation. *Horm Behav* 2008; **53**: 613–626.

16 Auyeung B, Baron-Cohen S, Ashwin E, Knickmeyer R, Taylor K, Hackett G *et al.* Fetal Testosterone Predicts Sexually Differentiated Childhood Behavior in Girls and in Boys. *Psychol Sci* 2009; **20**: 144–148.

17 Auyeung B, Ahluwalia J, Thomson L, Taylor K, Hackett G, O&amp KJ *et al.* Prenatal versus postnatal sex steroid hormone effects on autistic traits in children at 18 to 24 months of age. *Mol Autism* 2012; **3**: 17.

18 Knickmeyer R, Baron-Cohen S, Raggatt P, Taylor K. Foetal testosterone, social relationships, and restricted interests in children. *J Child Psychol Psychiatry* 2005; **46**: 198–210.

19 McKenna BG, Huang Y, K&eacute, Vervier V, Hofammann D, Cafferata M *et al.* Genetic and morphological estimates of androgen exposure predict social deficits in multiple neurodevelopmental disorder cohorts. *Mol Autism* 2021; **12**: 43.

20 Kung KTF, Spencer D, Pasterski V, Neufeld S, Glover V, O'Connor TG *et al.* No relationship between prenatal androgen exposure and autistic traits: convergent evidence from studies of children with congenital adrenal hyperplasia and of amniotic testosterone concentrations in typically developing children. *J Child Psychol Psychiatry* 2016; **57**: 1455–1462.

21 Xiong H, Peterson JB, Scott S. Amniotic testosterone and psychological sex differences: A systematic review of the extreme male brain theory. *Dev Rev* 2020; **57**: 100922.

22 O'Connor TG, Ciesla AA. Maternal Immune Activation Hypotheses for Human Neurodevelopment: Some Outstanding Questions. *Biol Psychiatry Cogn Neurosci Neuroimaging* 2022; **7**: 471–479.

23 Bucknor MC, Gururajan A, Dale RC, Hofer MJ. A comprehensive approach to modeling maternal immune activation in rodents. *Front Neurosci* 2022; **16**: 1071976.

24 Haddad FL, Patel SV, Schmid S. Maternal Immune Activation by Poly I:C as a preclinical Model for Neurodevelopmental Disorders: A focus on Autism and Schizophrenia. *Neurosci Biobehav Rev* 2020; **113**: 546–567.

25 Han VX, Patel S, Jones HF, Dale RC. Maternal immune activation and neuroinflammation in human neurodevelopmental disorders. *Nat Rev Neurol* 2021; **17**: 564–580.

26 Tioleco N, Silberman AE, Stratigos K, Banerjee-Basu S, Spann MN, Whitaker AH *et al.* Prenatal maternal infection and risk for autism in offspring: A meta-analysis. *Autism Res* 2021; **14**: 1296–1316.

27 Brynge M, Sjöqvist H, Gardner RM, Lee BK, Dalman C, Karlsson H. Maternal infection during pregnancy and likelihood of autism and intellectual disability in children in Sweden: a negative control and sibling comparison cohort study. *Lancet Psychiatry* 2022; **9**: 782–791.

28 Chang Y-C, Cole TB, Costa LG. Behavioral Phenotyping for Autism Spectrum Disorders in Mice. *Curr Protoc Toxicol* 2017; **72**: 11.22.1-11.22.21.

29 Haida O, Al Sagheer T, Balbous A, Francheteau M, Matas E, Soria F *et al.* Sex-dependent behavioral deficits and neuropathology in a maternal immune activation model of autism. *Transl Psychiatry* 2019; **9**: 1–12.

30 Malkova NV, Yu CZ, Hsiao EY, Moore MJ, Patterson PH. Maternal immune activation yields offspring displaying mouse versions of the three core symptoms of autism. *Brain Behav Immun* 2012; **26**: 607–616.

31 Careaga M, Murai T, Bauman MD. Maternal Immune Activation and Autism Spectrum Disorder: From Rodents to Nonhuman and Human Primates. *Biol Psychiatry* 2017; **81**: 391–401.

32 Choi GB, Yim YS, Wong H, Kim S, Kim H, Kim SV *et al.* The maternal interleukin-17a pathway in mice promotes autism-like phenotypes in offspring. *Science* 2016; **351**: 933–939.

33 Carlezon WA, Kim W, Missig G, Finger BC, Landino SM, Alexander AJ *et al.* Maternal and early postnatal immune activation produce sex-specific effects on autism-like behaviors and neuroimmune function in mice. *Sci Rep* 2019; **9**: 16928.

34 Cholemkery H, Medda J, Lempp T, Freitag CM. Classifying Autism Spectrum Disorders by ADI-R: Subtypes or Severity Gradient? *J Autism Dev Disord* 2016; **46**: 2327–2339.

35 Kim SY, Udhnani M, Lecavalier L. Heterogeneity in autism spectrum disorder explained by social-communicative and restricted repetitive behavior balance subgroups. *Res Autism Spectr Disord* 2024; **114**: 102387.

36 Zheng S, Hume KA, Able H, Bishop SL, Boyd BA. Exploring Developmental and Behavioral Heterogeneity among Preschoolers with ASD: A Cluster Analysis on Principal Components. *Autism Res* 2020; **13**: 796–809.

37 Sheng JA, Tobet SA. Maternal immune activation with toll-like receptor 7 agonist during mid-gestation alters juvenile and adult developmental milestones and behavior. *J Neuroendocrinol* 2024; **36**: e13417.

38 Cahill LS, Laliberté CL, Ellegood J, Spring S, Gleave JA, van Eede MC *et al.* Preparation of fixed mouse brains for MRI. *NeuroImage* 2012; **60**: 933–939.

39 Arbabi A, Spencer Noakes L, Vousden D, Dazai J, Spring S, Botelho O *et al.* Multiple-mouse magnetic resonance imaging with cryogenic radiofrequency probes for evaluation of brain development. *NeuroImage* 2022; **252**: 119008.

40 Zuo M, Fettig NM, Bernier L-P, Pössnecker E, Spring S, Pu A *et al.* Age-dependent gray matter demyelination is associated with leptomeningeal neutrophil accumulation. *JCI Insight* 2024; **9**: e183445.

41 Onore C, Careaga M, Ashwood P. The role of immune dysfunction in the pathophysiology of autism. *Brain Behav Immun* 2012; **26**: 383–392.

42 Ozaki K, Kato D, Ikegami A, Hashimoto A, Sugio S, Guo Z *et al.* Maternal immune activation induces sustained changes in fetal microglia motility. *Sci Rep* 2020; **10**: 21378.

43 Hu C, Li H, Li J, Luo X, Hao Y. Microglia: Synaptic modulator in autism spectrum disorder. *Front Psychiatry* 2022; **13**: 958661.

44 Xiong Y, Chen J, Li Y. Microglia and astrocytes underlie neuroinflammation and synaptic susceptibility in autism spectrum disorder. *Front Neurosci* 2023; **17**: 1125428.

45 Zhao H, Mao X, Zhu C, Zou X, Peng F, Yang W *et al.* GABAergic System Dysfunction in Autism Spectrum Disorders. *Front Cell Dev Biol* 2022; **9**: 781327.

46 Mangano GD, Riva A, Fontana A, Salpietro V, Mangano GR, Nobile G *et al. De novo GRIN2A* variants associated with epilepsy and autism and literature review. *Epilepsy Behav* 2022; **129**: 108604.

47 Mariggiò MA, Palumbi R, Vinella A, Laterza R, Petruzzelli MG, Peschechera A *et al.* DRD1 and DRD2 Receptor Polymorphisms: Genetic Neuromodulation of the Dopaminergic System as a Risk Factor for ASD, ADHD and ASD/ADHD Overlap. *Front Neurosci* 2021; **15**: 705890.

48 Yang F, You H, Mizui T, Ishikawa Y, Takao K, Miyakawa T *et al.* Inhibiting proBDNF to mature BDNF conversion leads to ASD-like phenotypes in vivo. *Mol Psychiatry* 2024; **29**: 3462–3474.

49 Ma K, Taylor C, Williamson M, Newton SS, Qin L. Diminished activity-dependent BDNF signaling differentially causes autism-like behavioral deficits in male and female mice. *Front Psychiatry* 2023; **14**: 1182472.

50 Dutra ML, Dias P, Freiberger V, Ventura L, Comim CM, Martins DF *et al.* Maternal immune activation induces autism-like behavior and reduces brain-derived neurotrophic factor levels in the hippocampus and offspring cortex of C57BL/6 mice. *Neurosci Lett* 2023; **793**: 136974.

51 Wang L, Zhou K, Fu Z, Yu D, Huang H, Zang X *et al.* Brain Development and Akt Signaling: the Crossroads of Signaling Pathway and Neurodevelopmental Diseases. *J Mol Neurosci* 2017; **61**: 379–384.

52 Hair JF, Tatham RL, Anderson RE, Black W. *Multivariate Data Analysis*. Pearson: Upper Saddle River, N.J, 1998.

53 Stevens JP, Stevens JP. *Applied Multivariate Statistics for the Social Sciences*. 4th edn Psychology Press: New York, 2001 doi:10.4324/9781410604491.

54 D'Amato FR, Scalera E, Sarli C, Moles A. Pups Call, Mothers Rush: Does Maternal Responsiveness Affect the Amount of Ultrasonic Vocalizations in Mouse Pups? *Behav Genet* 2006; **36**: 471–471.

55 Caruso A, Marconi MA, Scattoni ML, Ricceri L. Ultrasonic vocalizations in laboratory mice: strain, age, and sex differences. *Genes Brain Behav* 2022; **21**: e12815.

56 Banker SM, Gu X, Schiller D, Foss-Feig JH. Hippocampal contributions to social and cognitive deficits in autism spectrum disorder. *Trends Neurosci* 2021; **44**: 793–807.

57 Hui CW, Vecchiarelli HA, Gervais É, Luo X, Michaud F, Scheefhals L *et al.* Sex Differences of Microglia and Synapses in the Hippocampal Dentate Gyrus of Adult Mouse Offspring Exposed to Maternal Immune Activation. *Front Cell Neurosci* 2020; **14**: 558181.

58 Mohammadkhani R, Ghahremani R, Salehi I, Safari S, Karimi SA, Zarei M. Impairment in social interaction and hippocampal long-term potentiation at perforant pathway-dentate gyrus synapses in a prenatal valproic acid-induced rat model of autism. *Brain Commun* 2022; **4**: fcac221.

59 Baron-Cohen S, Auyeung B, Nørgaard-Pedersen B, Hougaard DM, Abdallah MW, Melgaard L *et al.* Elevated fetal steroidogenic activity in autism. *Mol Psychiatry* 2015; **20**: 369–376.

60 Spratt EG, Nicholas JS, Brady KT, Carpenter LA, Hatcher CR, Meekins KA *et al.* Enhanced cortisol response to stress in children in autism. *J Autism Dev Disord* 2012; **42**: 75–82.

61 Jouda J, Wöhr M, del Rey A. Immunity and ultrasonic vocalization in rodents. *Ann N Y Acad Sci* 2019; **1437**: 68–82.

62 Wöhr M, Scattoni ML. Behavioural methods used in rodent models of autism spectrum disorders: Current standards and new developments. *Behav Brain Res* 2013; **251**: 5–17.

63 Panksepp JB, Jochman KA, Kim JU, Koy JJ, Wilson ED, Chen Q *et al.* Affiliative Behavior, Ultrasonic Communication and Social Reward Are Influenced by Genetic Variation in Adolescent Mice. *PLoS ONE* 2007; **2**: e351–e351.

64 Peleh T, Eltokhi A, Pitzer C. Longitudinal analysis of ultrasonic vocalizations in mice from infancy to adolescence: Insights into the vocal repertoire of three wild-type strains in two different social contexts. *PLoS ONE* 2019; **14**: 1–19.

65 Xu X-J, Zhang H-F, Shou X-J, Li J, Jing W-L, Zhou Y *et al.* Prenatal hyperandrogenic environment induced autistic-like behavior in rat offspring. *Physiol Behav* 2015; **138**: 13–20.

66 Xiang D, Lu J, Wei C, Cai X, Wang Y, Liang Y *et al.* Berberine Ameliorates Prenatal Dihydrotestosterone Exposure-Induced Autism-Like Behavior by Suppression of Androgen Receptor. *Front Cell Neurosci* 2020; **14**: 87.

67 Yang M, Silverman JL, Crawley JN. Automated Three-Chambered Social Approach Task for Mice. *Curr Protoc Neurosci* 2011; **56**: Unit 8.26.

68 Matta SM, Hill-Yardin EL, Crack PJ. The influence of neuroinflammation in Autism Spectrum Disorder. *Brain Behav Immun* 2019; **79**: 75–90.

69 Loayza M, Lin S, Carter K, Ojeda N, Fan L-W, Ramarao S *et al.* Maternal immune activation alters fetal and neonatal microglia phenotype and disrupts neurogenesis in mice. *Pediatr Res* 2023; **93**: 1216–1225.

70 Mattei D, Ivanov A, Ferrai C, Jordan P, Guneykaya D, Buonfiglioli A *et al.* Maternal immune activation results in complex microglial transcriptome signature in the adult offspring that is reversed by minocycline treatment. *Transl Psychiatry* 2017; **7**: e1120–e1120.

71 Traetta ME, Tremblay M-È. Prenatal inflammation shapes microglial immune response into adulthood. *Trends Immunol* 2022; **43**: 953–955.

72 Bessis A, Béchade C, Bernard D, Roumier A. Microglial control of neuronal death and synaptic properties. *Glia* 2007; **55**: 233–238.

73 Lull ME, Block ML. Microglial activation and chronic neurodegeneration. *Neurotherapeutics* 2010; **7**: 354–365.

74 Colonna M, Butovsky O. Microglia Function in the Central Nervous System During Health and Neurodegeneration. *Annu Rev Immunol* 2017; **35**: 441–468.

75 Sati A, Prescott M, Holland S, Jasoni CL, Desroziers E, Campbell RE. Morphological evidence indicates a role for microglia in shaping the PCOS-like brain. *J Neuroendocrinol* 2021; **33**: 1–17.

76 Qin X-Y, Feng J-C, Cao C, Wu H-T, Loh YP, Cheng Y. Association of Peripheral Blood Levels of Brain-Derived Neurotrophic Factor With Autism Spectrum Disorder in Children: A Systematic Review and Meta-analysis. *JAMA Pediatr* 2016; **170**: 1079–1086.

77 Giovanoli S, Engler H, Engler A, Richetto J, Voget M, Willi R *et al.* Stress in Puberty Unmasks Latent Neuropathological Consequences of Prenatal Immune Activation in Mice. *Science* 2013; **339**: 1095–1099.

78 Mundorf A, Kubitza N, Hünten K, Matsui H, Juckel G, Ocklenburg S *et al.* Maternal immune activation leads to atypical turning asymmetry and reduced DRD2 mRNA expression in a rat model of schizophrenia. *Behav Brain Res* 2021; **414**: 113504.

79 Oh-Nishi A, Nagai Y, Seki C, Suhara T, Minamimoto T, Higuchi M. Imaging extra-striatal dopamine D2 receptors in a maternal immune activation rat model. *Brain Behav Immun - Health* 2022; **22**: 100446.

80 Saghazadeh A, Rezaei N. Systematic review and meta-analysis links autism and toxic metals and highlights the impact of country development status: Higher blood and erythrocyte levels for mercury and lead, and higher hair antimony, cadmium, lead, and mercury. *Prog Neuropsychopharmacol Biol Psychiatry* 2017; **79**: 340–368.

81 Barbosa AG, Pratesi R, Paz GSC, dos Santos MAAL, Uenishi RH, Nakano EY *et al.* Assessment of BDNF serum levels as a diagnostic marker in children with autism spectrum disorder. *Sci Rep* 2020; **10**: 17348.

82 Fanaei H, Karimian SM, Sadeghipour HR, Hassanzade G, Kasaeian A, Attari F *et al.* Testosterone enhances functional recovery after stroke through promotion of antioxidant defenses, BDNF levels and neurogenesis in male rats. *Brain Res* 2014; **1558**: 74–83.

83 Li M, Masugi-Tokita M, Takanami K, Yamada S, Kawata M. Testosterone has sublayer-specific effects on dendritic spine maturation mediated by BDNF and PSD-95 in pyramidal neurons in the hippocampus CA1 area. *Brain Res* 2012; **1484**: 76–84.

84 Rankov Petrovic B, Hrncic D, Mladenovic D, Simic T, Suvakov S, Jovanovic D *et al.* Prenatal Androgenization Induces Anxiety-Like Behavior in Female Rats, Associated with Reduction of Inhibitory Interneurons and Increased BDNF in Hippocampus and Cortex. *BioMed Res Int* 2019; **2019**: 1-12.

85 Purves-Tyson TD, Weber-Stadlbauer U, Richetto J, Rothmond DA, Labouesse MA, Polesel M *et al.* Increased levels of midbrain immune-related transcripts in schizophrenia and in murine offspring after maternal immune activation. *Mol Psychiatry* 2021; **26**: 849–864.

86 Gadow KD, Pinsonneault JK, Perlman G, Sadee W. Association of dopamine gene variants, emotion dysregulation and ADHD in autism spectrum disorder. *Res Dev Disabil* 2014; **35**: 1658–1665.

87 Hettinger JA, Liu X, Hudson ML, Lee A, Cohen IL, Michaelis RC *et al.* DRD2 and PPP1R1B (DARPP-32) polymorphisms independently confer increased risk for autism spectrum disorders and additively predict affected status in male-only affected sib-pair families. *Behav Brain Funct* 2012; **8**: 19.

88 Chhabra S, Nardi L, Leukel P, Sommer CJ, Schmeisser MJ. Striatal increase of dopamine receptor 2 density in idiopathic and syndromic mouse models of autism spectrum disorder. *Front Psychiatry* 2023; **14**: 1110525.

89 DiCarlo GE, Aguilar JI, Matthies HJG, Harrison FE, Bundschuh KE, West A *et al.* Autism-linked dopamine transporter mutation alters striatal dopamine neurotransmission and dopamine-dependent behaviors. *J Clin Invest* 2019; **129**: 3407–3420.

90 Maisterrena A, Matas E, Mirfendereski H, Balbous A, Marchand S, Jaber M. The State of the Dopaminergic and Glutamatergic Systems in the Valproic Acid Mouse Model of Autism Spectrum Disorder. *Biomolecules* 2022; **12**: 1691.

91 Hazlett HC, Poe M, Gerig G, Styner M, Chappell C, Smith RG *et al.* Early Brain Overgrowth in Autism Associated with an Increase in Cortical Surface Area Before Age 2. *Arch Gen Psychiatry* 2011; **68**: 467–476.

92 Khundrakpam BS, Lewis JD, Kostopoulos P, Carbonell F, Evans AC. Cortical Thickness Abnormalities in Autism Spectrum Disorders Through Late Childhood, Adolescence, and Adulthood: A Large-Scale MRI Study. *Cereb Cortex* 2017; **27**: 1721–1731.

93 Carper RA, Solders S, Treiber JM, Fishman I, Müller R-A. Corticospinal Tract Anatomy and Functional Connectivity of Primary Motor Cortex in Autism. *J Am Acad Child Adolesc Psychiatry* 2015; **54**: 859–867.

94 Courchesne E, Taluja V, Nazari S, Aamodt CM, Pierce K, Duan K *et al.* Embryonic origin of two ASD subtypes of social symptom severity: the larger the brain cortical organoid size, the more severe the social symptoms. *Mol Autism* 2024; **15**: 22-16.

95 Agam Y, Joseph RM, Barton JJS, Manoach DS. Reduced cognitive control of response inhibition by the anterior cingulate cortex in autism spectrum disorders. *NeuroImage* 2010; **52**: 336–347.

96 Thakkar KN, Polli FE, Joseph RM, Tuch DS, Hadjikhani N, Barton JJS *et al.* Response monitoring, repetitive behaviour and anterior cingulate abnormalities in autism spectrum disorders (ASD). *Brain* 2008; **131**: 2464–2478.

97 Walsh CP, Bovbjerg DH, Marsland AL. Glucocorticoid resistance and β2-adrenergic receptor signaling pathways promote peripheral pro-inflammatory conditions associated with chronic psychological stress: A systematic review across species. *Neurosci Biobehav Rev* 2021; **128**: 117–135.

98 Matthiesen M, Khlaifia A, Steininger CFD, Dadabhoy M, Mumtaz U, Arruda-Carvalho M. Maturation of nucleus accumbens synaptic transmission signals a critical period for the rescue of social deficits in a mouse model of autism spectrum disorder. *Mol Brain* 2023; **16**: 46.

99 Le Merrer J, Detraux B, Gandía J, De Groote A, Fonteneau M, de Kerchove d'Exaerde A *et al.* Balance Between Projecting Neuronal Populations of the Nucleus Accumbens Controls Social Behavior in Mice. *Biol Psychiatry* 2024; **95**: 123–135.

100 Higuchi Y, Tachigori S, Arakawa H. Faded neural projection from the posterior bed nucleus of the stria terminalis to the lateral habenula contributes to social signaling deficit in male BTBR mice as a mouse model of autism. *Psychoneuroendocrinology* 2023; **149**: 106004.

101 Contestabile A, Casarotto G, Musardo S, Espinosa P, Maltese F, Jiang Y *et al.* Shank3 deficits in the anteromedial bed nucleus of the stria terminalis trigger an anxiety phenotype in mice. *Eur J Neurosci* 2023; **57**: 1966–1979.

102 Yen T-L, Huang T-N, Lin M-H, Hsu T-T, Lu M-H, Shih P-Y *et al.* Sex bias in social deficits, neural circuits and nutrient demand in *Cttnbp2* autism models. *Brain* 2023; **146**: 2612–2626.

103 Jin S, Liu W, Hu Y, Liu Z, Xia Y, Zhang X *et al.* Aberrant functional connectivity of the bed nucleus of the stria terminalis and its age dependence in children and adolescents with social anxiety disorder. *Asian J Psychiatry* 2023; **82**: 103498.

104 Lebow MA, Chen A. Overshadowed by the amygdala: the bed nucleus of the stria terminalis emerges as key to psychiatric disorders. *Mol Psychiatry* 2016; **21**: 450–464.

105 Rein B, Raymond K, Boustani C, Tuy S, Zhang J, St. Laurent R *et al.* MDMA enhances empathy-like behaviors in mice via 5-HT release in the nucleus accumbens. *Sci Adv* 2024; **10**: eadl6554.

106 Guma E, Beauchamp A, Liu S, Levitis E, Ellegood J, Pham L *et al.* Comparative neuroimaging of sex differences in human and mouse brain anatomy. *eLife* 2024; **13**: RP92200.

107 Qiu LR, Fernandes DJ, Szulc-Lerch KU, Dazai J, Nieman BJ, Turnbull DH *et al.* Mouse MRI shows brain areas relatively larger in males emerge before those larger in females. *Nat Commun* 2018; **9**: 2615-15.

108 Swift-Gallant A, Monks DA. Androgenic mechanisms of sexual differentiation of the nervous system and behavior. *Front Neuroendocrinol* 2017; **46**: 32–45.

109 Tsompanidis A, Chang K, Khan Y, Radecki M, Dorfschmidt L, Hampton S *et al.* Perinatal brain growth and autistic traits in toddlers. 2025. Preprint at https://www.researchsquare.com/article/rs-5462151/v1.

110 Minakova E, Warner BB. Maternal immune activation, central nervous system development and behavioral phenotypes. *Birth Defects Res* 2018; **110**: 1539–1550.

111 Zhang S, Ding J, Wang J, Yin T, Zhang Y, Yang J. CXCL5 Downregulation in Villous Tissue Is Correlated With Recurrent Spontaneous Abortion. *Front Immunol* 2021; **12**: 717483.

112 Zhang S, Ding J, Zhang Y, Liu S, Yang J, Yin T. Regulation and Function of Chemokines at the Maternal–Fetal Interface. *Front Cell Dev Biol* 2022; **10**: 826053.

113 Mastenbroek LJM, Kooistra SM, Eggen BJL, Prins JR. The role of microglia in early neurodevelopment and the effects of maternal immune activation. *Semin Immunopathol* 2024; **46**: 1.

114 Woods RM, Lorusso JM, Fletcher J, ElTaher H, McEwan F, Harris I *et al.* Maternal immune activation and role of placenta in the prenatal programming of neurodevelopmental disorders. *Neuronal Signal* 2023; **7**: NS20220064.

115 Carpentier PA, Dingman AL, Palmer TD. Placental TNF-α Signaling in Illness-Induced Complications of Pregnancy. *Am J Pathol* 2011; **178**: 2802–2810.

116 Fujitani M, Miyajima H, Otani Y, Liu X. Maternal and Adult Interleukin-17A Exposure and Autism Spectrum Disorder. *Front Psychiatry* 2022; **13**: 836181.

117 Glassman CR, Su L, Majri-Morrison SS, Winkelmann H, Mo F, Li P *et al.* Calibration of cell-intrinsic interleukin-2 response thresholds guides design of a regulatory T cell biased agonist. *eLife* 2021; **10**: e65777.

118 Osman I, Young A, Ledingham MA, Thomson AJ, Jordan F, Greer IA *et al.* Leukocyte density and pro-inflammatory cytokine expression in human fetal membranes, decidua, cervix and myometrium before and during labour at term. *Mol Hum Reprod* 2003; **9**: 41–45.

119 Zhao H, Zhang H, Liu S, Luo W, Jiang Y, Gao J. Association of Peripheral Blood Levels of Cytokines With Autism Spectrum Disorder: A Meta-Analysis. *Front Psychiatry* 2021; **12**: 670200.

120 Cesta CE, Öberg AS, Ibrahimson A, Yusuf I, Larsson H, Almqvist C *et al.* Maternal polycystic ovary syndrome and risk of neuropsychiatric disorders in offspring: prenatal androgen exposure or genetic confounding? *Psychol Med* 2020; **50**: 616–624.

121 Cherskov A, Pohl A, Allison C, Zhang H, Payne RA, Baron-Cohen S. Polycystic ovary syndrome and autism: A test of the prenatal sex steroid theory. *Transl Psychiatry* 2018; **8**: 136–10.

122 Kosidou K, Dalman C, Widman L, Arver S, Lee BK, Magnusson C *et al.* Maternal polycystic ovary syndrome and the risk of autism spectrum disorders in the offspring: a population-based nationwide study in Sweden. *Mol Psychiatry* 2016; **21**: 1441–1441.

123 Palomba S, Marotta R, Di Cello A, Russo T, Falbo A, Orio F *et al.* Pervasive developmental disorders in children of hyperandrogenic women with polycystic ovary syndrome: a longitudinal case-control study. *Clin Endocrinol Oxf* 2012; **77**: 898–904.

124 Sir-Petermann T, Maliqueo M, Angel B, Lara HE, Pérez-Bravo F, Recabarren SE. Maternal serum androgens in pregnant women with polycystic ovarian syndrome: possible implications in prenatal androgenization. *Hum Reprod Oxf* 2002; **17**: 2573–2579.

125 Kelley AS, Smith YR, Padmanabhan V. A Narrative Review of Placental Contribution to Adverse Pregnancy Outcomes in Women With Polycystic Ovary Syndrome. *J Clin Endocrinol Amp Metab* 2019; **104**: 5299–5316.

126 Nisenblat V, Norman RJ. Androgens and polycystic ovary syndrome. *Curr Opin Endocrinol Diabetes Obes* 2009; **16**: 224–231.

127 Vacher C-M, Tsompanidis A, Firestein MR, Penn AA. Neuroactive steroid exposure impacts neurodevelopment: Comparison of human and rodent placental contribution. *J Neuroendocrinol* 2025; **37**: e13489.

128 Dimova T, Alexandrova M, Vangelov I, You Y, Mor G. The modeling of human implantation and early placentation: achievements and perspectives. *Hum Reprod Update* 2025; **31**: 133–163.

129 Bonthuis PJ, Cox KH, Searcy BT, Kumar P, Tobet S, Rissman EF. Of mice and rats: key species variations in the sexual differentiation of brain and behavior. *Front Neuroendocrinol* 2010; **31**: 341–358.

130 Riede T, Borgard HL, Pasch B. Laryngeal airway reconstruction indicates that rodent ultrasonic vocalizations are produced by an edge-tone mechanism. *R Soc Open Sci* 2017; **4**: 170976.

131 Jamnadass ESL, Keelan JA, Hollier LP, Hickey M, Maybery MT, Whitehouse AJO. The perinatal androgen to estrogen ratio and autistic-like traits in the general population: a longitudinal pregnancy cohort study. *J Neurodev Disord* 2015; **7**: 17.

132 Whitehouse AJ, Mattes E, Maybery MT, Dissanayake C, Sawyer M, Jones RM *et al.* Perinatal testosterone exposure and autistic-like traits in the general population: a longitudinal pregnancy-cohort study. *J Neurodev Disord* 2012; **4**: 25.

Figures

Figure 1

a) Experimental timeline for juvenile animals

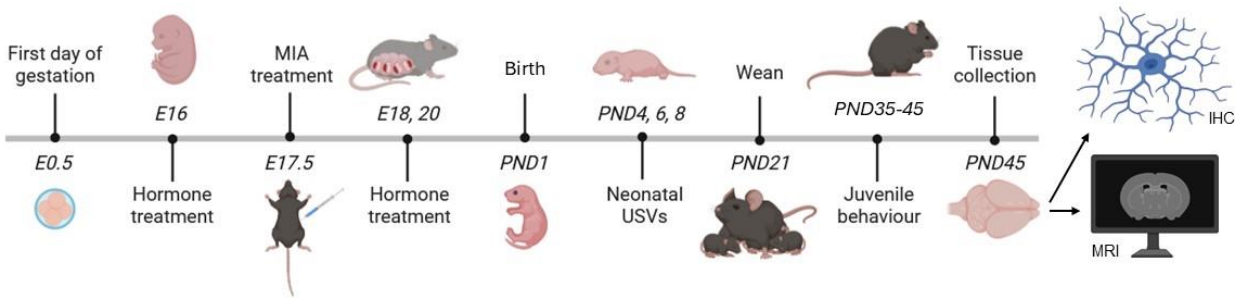

b) Experimental timeline for fetal and neonatal animals

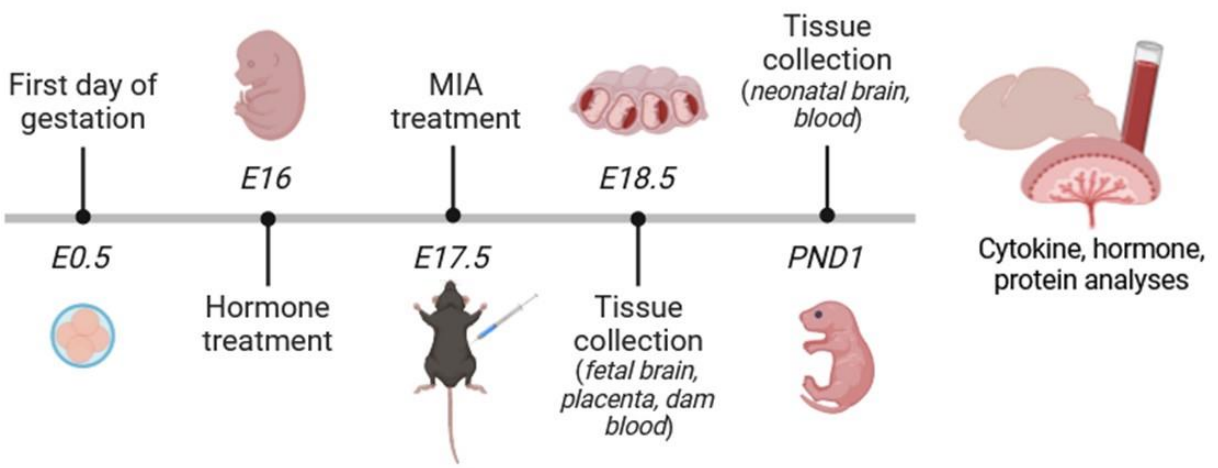

a) The presence of a seminal plug marked embryonic day (E) 0.5. MIA treatment (poly I:C or saline vehicle) was administered to mouse dams on E17.5 via I.P. injection. Hormone treatment (TP or oil vehicle) was administered subcutaneously to dams on E16, 18, and 20, and to pups on postnatal day (PND) 1. Neonatal USVs were recorded on PND 4, 6, and 8 in response to a three-minute isolation from the nest. Offspring were weaned on PND 21. Juvenile behaviors, namely USVs (same- or opposite-sex stimulus animal), marble burying, and three-chamber social paradigm, were performed between PND 35-45. Offspring were overdosed and decapitated on PND 45 for tissue collection. Magnetic resonance imaging (MRI) was performed for a subset of brain tissue, with another subset used for microglia analysis via immunohistochemistry (IHC). b) Male fetuses and placentas were removed from the uterine horn on E18.5 and brains were extracted. For neonatal samples, pups were rapidly decapitated on the day of birth and brains and bloods were collected. Cytokine, hormone, and protein analyses were conducted on fetal and neonatal tissue samples. Note: hormone treatment to hyperandrogenized dams for fetuses and neonate experiment were only exposed to testosterone on E16 and E18, while hyperandrogenized dams for offspring that were survived past the day of birth, were administered testosterone on E16, E18 and PND1. *Figure created with BioRender.com.*

Figure 2. *Neonatal ultrasonic vocalizations (PND 4–8) and juvenile social, communicative, and repetitive behaviors*

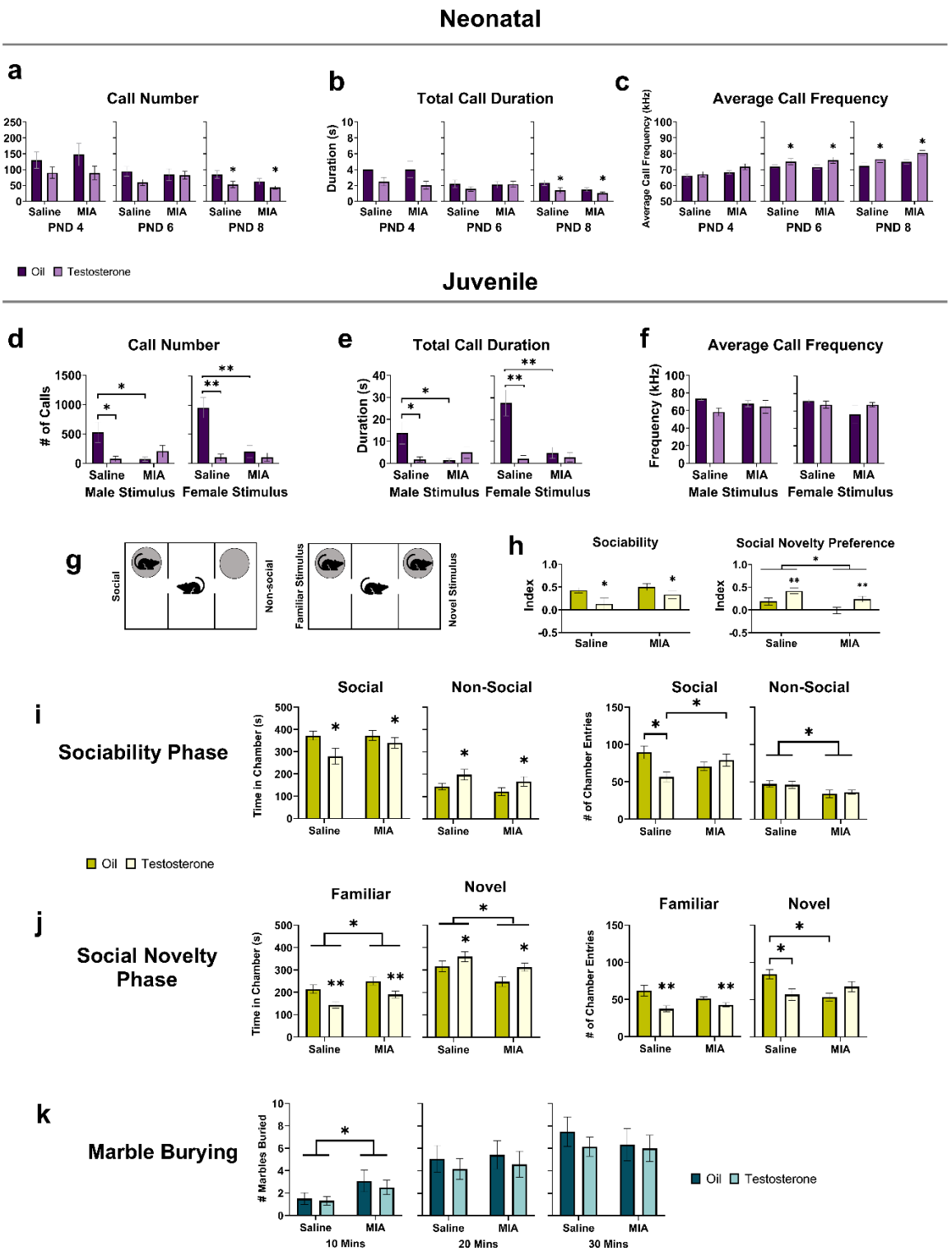

a) At PND 6 and 8, hyperandrogenized pups called at a higher frequency than controls (hormone treatment effect; MANOVA: PND 6 $F_{4,42} = 2.95$, $p = .031$; PND 8 $F_{4,44} = 4.03$, $p = .007$; univariate ANOVAs: PND 6 $F_{1, 45} = 4.86$, $p = .033$; PND 8 $F_{1, 47} = 7.65$, $p = .008$). b) At PND 8, hyperandrogenized pups produced fewer calls than controls (univariate ANOVA: $F_{1, 47} = 6.93$, $p = .011$). c) Hyperandrogenized pups spent less time calling than controls at PND 8 (univariate ANOVA: $F_{1, 47} = 6.74$, $p = .013$). d) Hyperandrogenized and MIA mice produced fewer calls than oil-treated saline controls during encounters with a same-sex stimulus (MANOVA: $F_{4,34} = 2.96$, $p = .034$; call number: $F_{1,37} = 6.28$, $p = .017$; hyperandrogenized vs control: $p = .009$, $d = 1.216$; MIA vs control: $p = .007$, $d = 1.226$) or opposite-sex stimulus (MANOVA: $F_{4,34} = 2.93$, $p = .035$; call number: $F_{1,37} = 12.51$, $p = .001$, $d = 0.950$; hormone treatment effect: MANOVA: $F_{4,34} = 4.80$, $p = .004$; call number: $F_{1,37} = 15.11$, $p < .001$, $d = 1.207$). e) Both hyperandrogenized and MIA mice spent less time calling than controls when encountering a same-sex stimulus (total call duration: $F_{1,37} = 5.57$, $p = .024$; hyperandrogenized vs control: $p = .014$, $d = 1.139$; MIA vs control: $p = .009$, $d = 1.178$) or opposite-sex stimulus (total call duration: $F_{1,37} = 11.03–12.64$, $p = .002–.001$; MIA vs control: $d = 0.892$; hormone treatment vs control: $d = 1.103$). No significant differences were found between groups for average call duration or f) frequency during same- or opposite-sex encounters (p's > .05). g) Three-chamber social paradigm apparatus depicting set-up for tests of sociability (social and non-social chambers) and social novelty preference (familiar stimulus and novel stimulus chambers). h) Hyperandrogenized mice had a lower sociability index than controls (effect hormone treatment, $F_{1, 45} = 6.259$, $p = .016$). MIA groups had a reduced social novelty preference than controls (MIA effect, $F_{1, 45} = 7.470$, $p = .009$). Hyperandrogenized offspring had a greater social novelty preference than controls (hormone treatment, $F_{1, 45} = 12.566$, $p < .001$). i) Hyperandrogenized animals spent less time in the social chamber and more time in the non-social chamber than controls (hormone treatment, $F_{1, 45} = 5.404$, $p = .025$). Hyperandrogenized mice entered the social chamber less often than controls (saline/oil) and hyperandrogenized MIA mice (MIA X hormone treatment, $F_{1, 45} = 8.193$, $p = .006$). MIA animals entered the non-social chamber less than controls (MIA effect, $F_{1, 45} = 7.025$, $p = .011$). j) MIA animals spent more time in the familiar stimulus chamber and less time in the novel stimulus chamber compared to controls (MIA effect [familiar stimulus, $F_{1, 45} = 6.464$, $p = .015$; novel stimulus, $F_{1, 45} = 7.092$, $p = .011$]). Hyperandrogenized animals spent less time in the familiar stimulus chamber and more time in the novel stimulus chamber compared to controls (hormone treatment: [familiar stimulus, $F_{1, 45} = 15.756$, $p < .001$; novel stimulus, $F_{1, 45} = 6.244$, $p = .016$]). MIA and hyperandrogenized mice entered the novel stimulus chamber less than controls (MIA X hormone treatment, $F_{1, 45} = 9.715$, $p = .003$). Hyperandrogenized animals entered familiar stimulus chamber less than controls (hormone treatment, $F_{1, 45} = 13.104$, $p < .001$). k) Interaction between number of marbles buried across time and MIA treatment, $F_{2, 90} = 12.83$, $p = .040$. At 10-minute timepoint, MIA mice buried significantly more marbles than controls, $p = .042$. *Note*. *$p < .05$, **$p < .001$. Data are shown as mean ± SEM.

Figure 3. *Ex vivo magnetic resonance imaging*

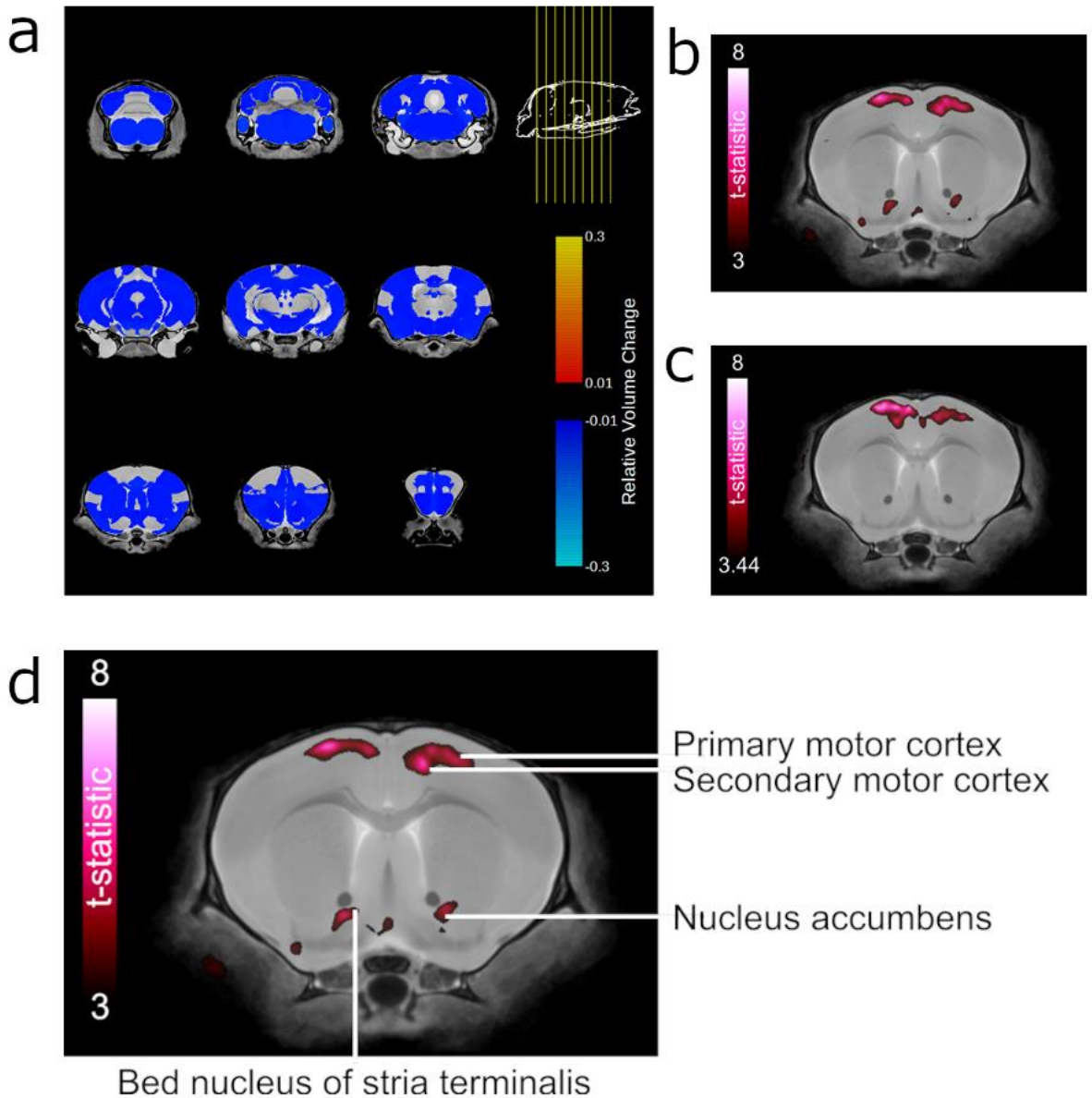

a) Coronal sections depict relative volume changes in juvenile hyperandrogenized brains compared to controls. Voxel-wise analyses revealed reduced volumes in highlighted regions in hyperandrogenized mice (15% FDR). b) Coronal section depicts the areas (primary and secondary motor cortex, BNST and nucleus accumbens) that are relatively larger (normalized to total brain volume) in hyperandrogenized vs control brains (t-statistic = 2.99, 15% FDR). **c)** Coronal section depicting the areas (cingulate cortex, primary and secondary motor cortex) that are larger in MIA compared to control brains (t-statistic = 3.44, 15% FDR). d) Labelled coronal section depicting regions that are relatively larger in hyperandrogenized vs control brains.

Figure 4. *Immunological, endocrine, and gene expression profiles in hyperandrogenization and MIA models*

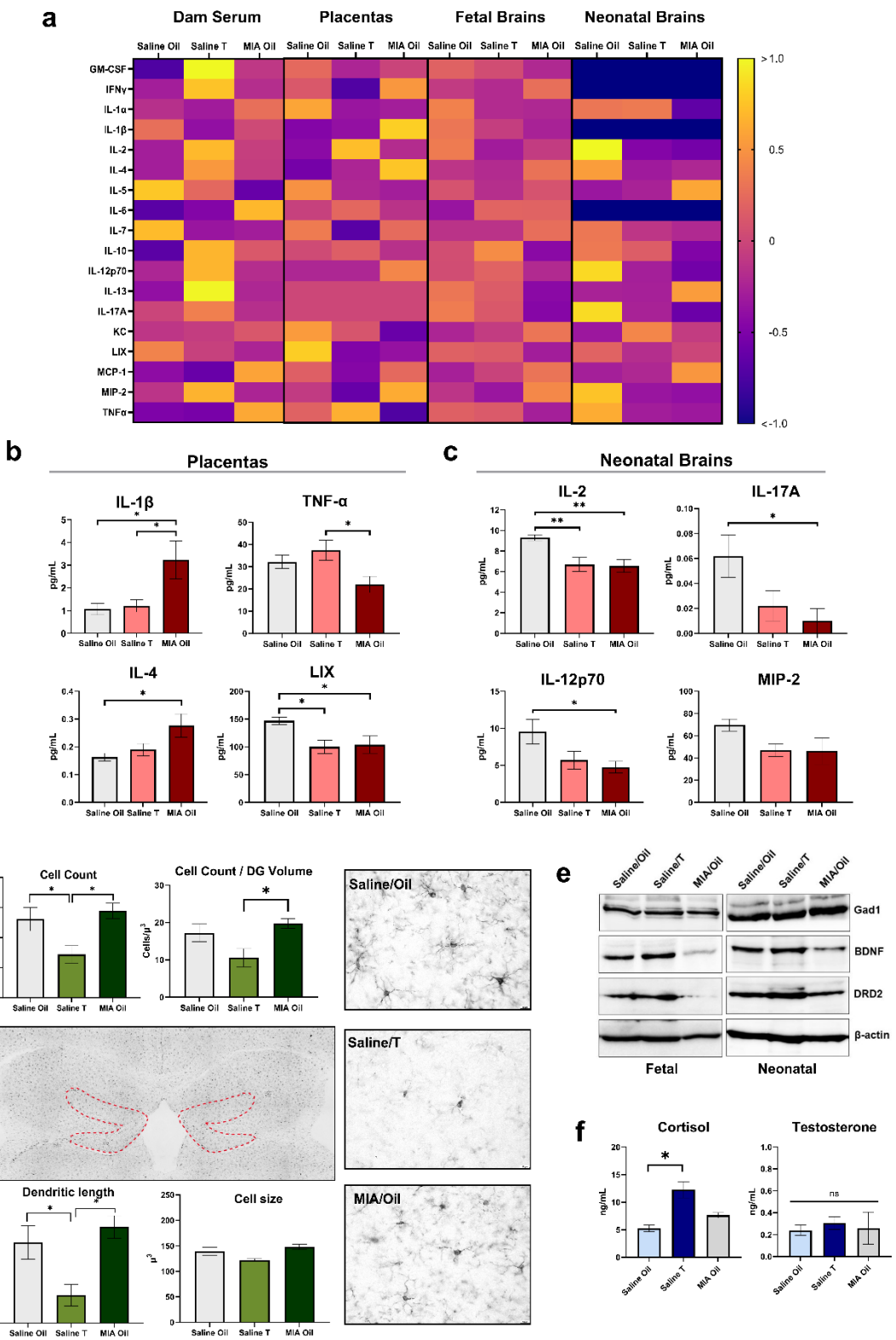

a) Heat map depicting z-scores of cytokine concentrations in dam serum, placenta, fetal brains, and neonatal brains. b) In placental tissue, levels of LIX ($F_{2,17} = 4.757$, $p = .023$) were reduced in MIA ($p = .019$) and hyperandrogenized ($p = .015$) mice compared to controls. MIA placentas had higher levels of IL-4 than controls ($F_{2,17} = 4.351$, $p = .011$). IL-1β ($F_{2,17} = 4.939$, $p = .020$) was higher in MIA mice compared to hyperandrogenized ($p = .021$) and controls ($p = .011$) Levels of TNF-α ($F_{2,17} = 4.411$, $p = .029$) were lower in MIA compared to hyperandrogenized mice $p = .010$). c) In neonatal brains, levels of IL-2, IL-17A, and IL-12p70 were significantly lower in MIA mice compared to controls ($F_{2,12} = 4.037$- 7.698, $p = .004$-$.020$). IL-2 was also lower in hyperandrogenized offspring compared to controls ($F_{2,12} = 7.698$, $p = .006$). d) Microglia were assessed in the hippocampal dentate gyrus (DG) (outlined in red) of juvenile offspring. Representative images of microglia in the DG of saline-oil, saline-T, and MIA-oil mice. Hyperandrogenized mice had reduced microglial cell counts compared to MIA and controls ($F_{2,12} = 4.422$, $p = .036$). MIA mice had a greater cell count / DG volume compared to hyperandrogenized mice ($F_{2,12} = 4.296$, $p = .039$). Dendritic length of microglia were shorter in hyperandrogenized mice compared to MIA and controls ($F_{2,12} = 5.405$, $p = .021$). Cell size did not differ between groups (p's > .05). e) Western blots showing the expression of Gad1, BDNF, and DRD2 from the protein lysates of fetal and neonatal mouse brain tissues. β-actin was used as a loading control. f) Neonatal hyperandrogenized saline offspring had higher concentrations of cortisol in serum compared to MIA-testosterone and saline-oil offspring (MIA X hormone treatment interaction, $F_{1,8} = 28.939$, $p < .001$). Groups did not differ for testosterone concentrations (p's > .05). *Note*. *$p < .05$, **$p < .001$. Data are shown as mean ± SEM.

Figure 5. *Developmental trajectories underlying the distinct ASD-like phenotype in the hyperandrogenization and MIA preclinical ASD models*

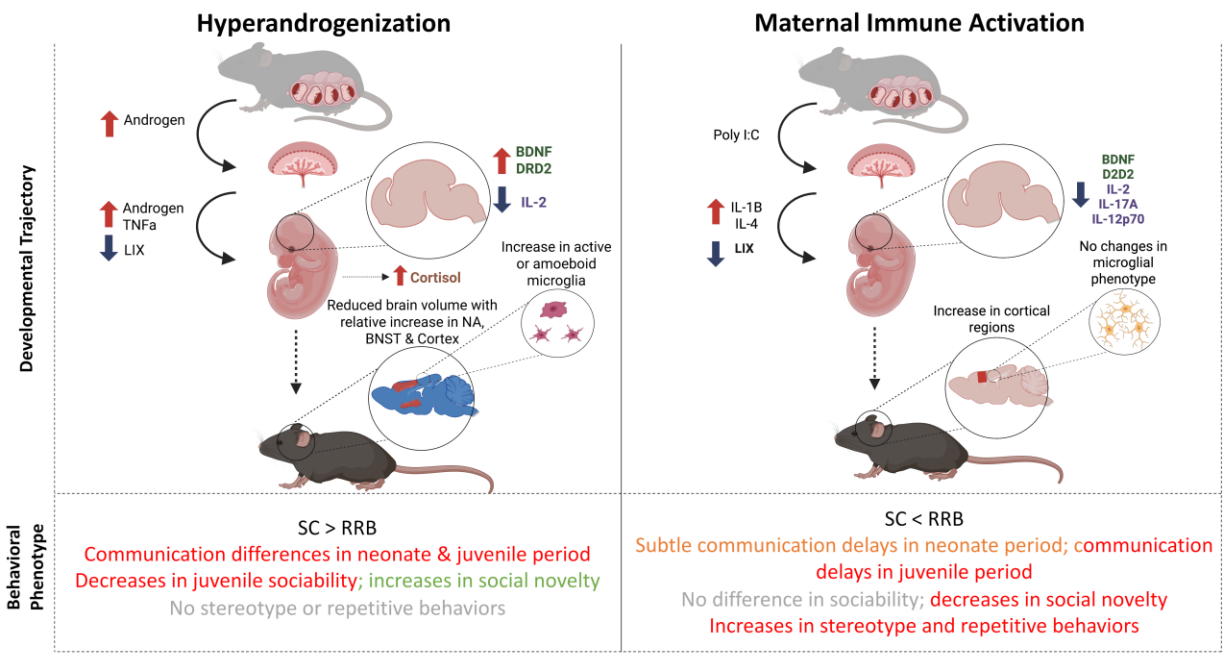

With perinatal hyperandrogenization, fetal development is influenced by both the high androgen exposure and pro-inflammatory cytokines from the placenta (i.e., TNFα increased, reduced LIX). This results in high BDNF and DRD2 protein levels in fetal brains, reduced IL-2 in neonate brains, and persistent evidence of neuroinflammation (microglia) in juveniles, likely contributing to the overall reduction in brain volume in this model. In contrast, MIA led to reductions in LIX compared to controls, and heightened placental IL-1B and IL-4, and decreased IL-2, IL-17A, IL-12p70 and BDNF/DRD2 in neonatal brains. In the MIA model, there were no overall changes to brain volume, or microglia quantity or quality, though there were increases in cortical regions (motor cortices, cingulate cortex) compared to controls. These two factors associated with ASD likelihood, hyperandrogenization and MIA, lead to distinctive patterns of neurodevelopment, and these two models map onto distinct subtypes of ASD based on social communication (SC) vs repetitive-restricted behavior (RRB) domains. Created in BioRender. Swift-Gallant, A. (2025) https://BioRender.com/omqk91p

Tables

Table 1. *Significant change in absolute volume of brain structures between saline testosterone (n = 8) compared to saline oil (n = 8) at 6 weeks of age.*

Structure	Change in absolute volume (%)	Groupwise absolute volume differences uncorrected *p*-value
Anterior commissure: pars anterior	-3.1	0.005**
Anterior commissure: pars posterior	-3.4	0.004**
Bed nucleus of stria terminalis	-3.5	0.02*
Cerebellar peduncle: inferior	-5.4	0.008**
Cerebellar peduncle: middle	-6.2	0.009**
Cerebral peduncle	-5.1	0.01**
Cerebellum:		
Lobule VI	-3.1	0.04*
Lobule IX	-2.5	0.05*
Lobule X	-4.4	0.05*
Anterior lobule (lobules 4-5)	-6.5	0.02*
Crus I (lobule 6)	-4.0	0.05*
Flocculus	-6.7	0.0003***
Lobules IV-V white matter	-2.7	0.004**
Anterior lobule white matter	-7.9	0.05*
Simple lobule white matter	-6.8	0.008**
Crus I white matter	-2.8	0.04*
Crus II white matter	-2.4	0.05*
Paraflocculus white matter	-7.1	0.02**
Corpus callosum	-5.1	0.005**
Cortex:		
Cingulate cortex: Area 24a	-5.8	0.02*
Cingulate cortex: Area 24a’	-3.2	0.03*
Cingulate cortex: Area 29b	-4.4	0.03*
Primary auditory cortex	-4.6	0.05*
Dorsal tenia tecta	-3.8	0.02*
Intermediate nucleus of the endopiriform	-3.9	0.05*
claustrum	-4.9	0.006**
Lateral orbital cortex	-2.3	0.03*
Primary motor cortex	-5.5	0.05*
Medial orbital cortex	-4.6	0.03*
Perirhinal cortex	-3.2	0.03*
Parietal cortex (posterior area)	-3.5	0.0002***
Primary somatosensory cortex (dysgranular zone)	-3.4	0.02**
Primary somatosensory cortex (forelimb region)	-3.1	0.05*
Primary somatosensory cortex (hindlimb region)	-4.4	0.01**
Primary somatosensory cortex (jaw region)	-3.8	0.03*
Primary somatosensory cortex (trunk region)	-3.8	0.0007***
Primary somatosensory cortex (upper lip region)	-4.3	0.04*

Primary visual cortex	-3.9	0.05*
Secondary visual cortex (lateral area)	-3.6	0.05*
Ventral intermediate entorhinal cortex	-3.9	0.01**
Ventral orbital cortex		
Facial nerve (cranial nerve 7)	-7.3	0.04*
Fornix	-3.9	0.05*
Globus pallidus	-3.3	0.01**
Habenular commissure	-11.7	0.04*
Hippocampus:		
CA1 oriens layer	-4.2	0.04*
CA1 lacunosum moleculare layer	-3.7	0.05*
CA2 pyramidal layer	-2.2	0.04*
CA2 oriens layer	-2.4	0.03*
CA2 radiatum layer	-2.3	0.05*
Molecular layer of dentate gyrus	-3.9	0.04*
Polymorph layer of dentate gyrus	-3.8	0.04*
Hypothalamus	-3.2	0.008**
Internal capsule	-4.7	0.02*
Lateral septum	-4.3	0.05*
Mammilothalamic tract	-3.7	0.004**
Medial septum	-2.5	0.01**
Nucleus accumbens	-3.0	0.01**
Olfactory bulb:		
Lateral olfactory tract	-2.4	0.0004***
Olfactory peduncle	-2.6	0.005**
Olfactory bulb (external plexiform layer)	-4.6	0.003**
Olfactory bulb (mitral cell layer)	-4.2	0.02*
Olfactory bulb (internal plexiform layer)	-3.5	0.008**
Olfactory bulb (granule cell layer)	-2.9	0.006**
Accessory olfactory bulb (glomerular external plexiform and mitral cell layer)	-2.1	0.05*
Anterior olfactory nucleus	-2.8	0.01**
Optic tract	-3.7	0.01**
Stria terminalis	-4.7	0.02*
Striatum	-3.7	0.04*
Subependymale zone/rhinocele	-4.5	0.01**
Subiculum	-4.2	0.006**
Superior olivary complex	-5.1	0.007**
Third ventricle	-5.9	0.006**

* FDR = 15%, ** FDR = 10%, *** FDR = 5%

Note: Crus II white matter and paramedian lobule in the cerebellum and the olfactory tubercle have greater asymmetry in the hyperandrogenized vs control brains. For the behavioural tests, correlations were conducted for brain structures that were decreased in the hyperandrogenized group compared to controls. For the three-chamber test, the cerebral peduncle and superior olivary complex showed a positive correlation with social chamber time for the control group

while there was no correlation for the hyperandrogenized group ($p = 0.03$). For the open field test, the mammilothalamic tract and lobule X of the cerebellum showed a positive correlation with the outer zone entries for the controls ($p = .04$) while there was no correlation for the hyperandrogenized group.